All-Star Polymer Multilayers as pH-Responsive Nanofilms

Byeong-Su Kim,[†] Haifeng Gao,[‡] Avni A. Argun,[†] Krzysztof Matyjaszewski,*[,‡] and Paula T. Hammond*[,†]

Department of Chemical Engineering, Institute for Soldier Nanotechnologies, Massachusetts Institute of Technology, 77 Massachusetts Avenue, Cambridge, Massachusetts 02139, and Department of Chemistry, Carnegie Mellon University, 4400 Fifth Avenue, Pittsburgh, Pennsylvania 15213

Received August 7, 2008; Revised Manuscript Received November 12, 2008

ABSTRACT: Star polymers with globular architecture and multiple arms are among the simplest forms of polymers with branched topologies. The combination of their unique architecture and high local densities of active functional groups makes star polymers unique candidates for a diverse range of applications. In this article, we describe the synthesis of star polymers with precisely controlled structures via atom transfer radical polymerization (ATRP) using the one-pot arm-first method. Specifically, two types of highly defined, high charge density star polymers with oppositely charged arm structures were prepared: poly[2-(dimethylamino)ethyl methacrylate] (PDMAEMA) star and poly(acrylic acid) (PAA) star polymers with cross-linked cores. By exploiting the electrostatic interactions between the polyelectrolyte arms, we have integrated the PDMAEMA star and PAA star polymers within alternating multilayer thin films using layer-by-layer (LbL) assembly to generate all-star polyelectrolyte LbL films. The prepared star/star multilayer films illustrate nonuniform and nanoporous structures, which result from the characteristic architecture of star polymers. The thickness, porosity, and refractive index of star/star multilayer films are precisely tunable by assembly pH conditions. Furthermore, as-assembled star/star multilayer films exhibit distinct morphological changes by undergoing extensive structural reorganization upon post-treatment under different pH conditions that do not lead to any changes with their linear compositional counterparts; it is hypothesized that these differences are due to the star polyelectrolyte's compact structure and decreased extent of entanglement and interpenetration, which lead to a low degree of ionic cross-linking compared to their linear counterparts. The pH-responsive structural changes of the films are characterized by AFM, SEM, and FTIR. Finally, we have observed an enhanced ionic (proton) conductivity of star/star multilayers following the pH-induced structural reorganization.

Introduction

Layer-by-layer (LbL) assembly has been widely employed as a simple, yet versatile, method in constructing controlled nanostructures on a surface.[1−4] It allows the creation of highly tunable, functional thin films with nanometer-level control over the structure, composition, and properties. With new advances, a wide variety of materials have been explored as active building blocks for LbL assembly beyond simple polyelectrolytes, including inorganic nanoparticles,[5] polymeric micelles,[6] dendrimers,[7,8] carbon nanotubes,[9] and biological molecules.[10] The incorporation of a broader range of materials based on the various intermolecular interactions has expanded the potential applications of LbL assembly ranging from energy and electrochemical devices to drug delivery platforms.[11−17] As new nanoscale materials are introduced and developed as active components in LbL assembly, it would be of general interest to investigate the structural and morphology effects of LbL films that contain polymers with unusual architecture and functionalities compared to conventional polyelectrolytes. The general phenomena that have been reported for linear systems may not be as applicable to systems in which the polymer chains are more constrained or for which the average size and shape of the macromolecules are unique. Ultimately, such differences may lead to differences in film density, morphology, mechanical properties, pH, and other stimuli-responsive behavior that would be of significant interest for all of the applications described above. This study will be of importance in understanding the fundamental behavior of star polymers within multilayers and their potential applications as active building blocks in LbL multilayer films. Finally, comparisons between linear−linear and star−star multilayer systems with equivalent compositions can elucidate greater understanding of the nature of ionic self-assembly in these films.

Star polymers with a globular shape and multiple arms connecting at a central core are among the simplest forms of branched topologies.[18] In comparison to their linear analogues, star polymers have different rheological and mechanical properties and possess a significantly higher degree of functionalities.[19] It is important to note that globular star polymers can be used as an analogue to dendrimers for many applications with far less synthetic cost and challenges. Recent advances in the synthetic opportunities offered by various controlled/living radical polymerization (CRP)[20−22] techniques have demonstrated successful preparation of star polymers with a variety of structures and functionalities. Atom transfer radical polymerization (ATRP),[23−25] one of the most popular CRP techniques, has been widely used for the synthesis of star polymers by one of three strategies: core-first,[26−29] coupling-onto,[30,31] and arm-first method.[32−35] For example, star polymers with controlled structures have been synthesized via ATRP using the one-pot arm-first method in this study.[35] The combination of various structural conformations and dimensions and high local densities of active functional groups makes star polymers unique candidates for a diverse range of applications, including surface engineering, novel responsive materials, and drug delivery. The integration of star polymers into polymeric thin films on surfaces has been recently demonstrated by a few groups. For example, Chen and co-workers have reported a multilayer formation based on a poly(acrylic acid) (PAA) star polymer with an inorganic precursor core.[36] Similarly, Qiao and co-workers have recently shown the incorporation of PAA star polymers within LbL assembled polymeric multilayers and their pH-responsive

* Corresponding authors. E-mail: km3b@andrew.cmu.edu, hammond@mit.edu.
[†] Massachusetts Institute of Technology.
[‡] Carnegie Mellon University.

10.1021/ma801812v CCC: $40.75
Published on Web 12/05/2008

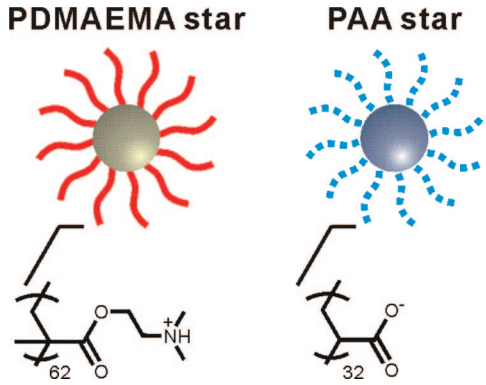

Figure 1. Chemical structures of multilayered PDMAEMA and PAA star polymers utilizing the electrostatic interactions. The weight-average molecular weight of arm, $M_{w,arm}$, of PDMAEMA star is 9670 g/mol, and $M_{w,arm}$ of the PAA star is 2310 g/mol. The average number of arms, n_{arm}, of PDMAEMA star and PAA star is 19 and 24, respectively.

Scheme 1. General Synthetic Scheme for the Star Polymers by the Arm-First ATRP Method

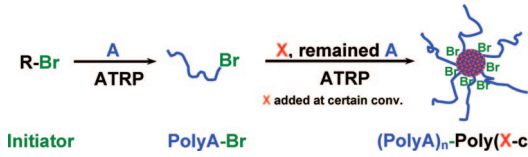

surface properties.[37] Although both studies have taken advantage of the unique geometry of star polymers, they have still incorporated a coil-like linear counter-polyion in the assembly of thin films. Here we show that star polymers can be unique building blocks in multilayer film formation, with structural and functional characteristics that are absent in most of their linear counterparts.

In this report, we introduce *the first example* of ultrathin multilayer films exclusively based on star polymers. We show that we can precisely control the thickness and composition of these films. The primary aim of this report is to demonstrate the preparation of star polymers and their integration into multilayers by means of LbL assembly. Specifically, arm−core type star polymers with oppositely charged polyelectrolyte arms and cross-linked cores were synthesized via ATRP with the one-pot arm-first method.[35] The star/star multilayer was then assembled by sequential LbL deposition exploiting electrostatic interactions between star polymers with positively charged poly[2-(dimethylamino)ethyl methacrylate] (PDMAEMA) arms and negatively charged poly(acrylic acid) (PAA) arms (Figure 1). The assembly behavior of the system, compared to conventional linear polyelectrolytes, is also demonstrated. Furthermore, we have discovered an unusually high tendency toward pH-responsive morphological rearrangements in star/star multilayer films due to the changes in ionization of the polyelectrolytes and the distinctive geometry of star polymers.

Experimental Methods

Materials. The PDMAEMA and PAA star polymers were prepared according to a previously published paper by using the one-pot arm-first process (Scheme 1).[35] Briefly, the PDMAEMA star polymer was synthesized first by ATRP reaction of 2-(dimethylamino)ethyl methacrylate (DMAEMA) as a monomer to afford linear PDMAEMA macroinitiators with active bromine chain-end functional groups. Subsequently, linear PMDAEMA macroinitiators were cross-linked via addition of ethylene glycol dimethacrylate (EGDMA) cross-linker to the reaction system at certain DMAEMA conversion. This afforded the formation of arm-core type polymers of poly(DMAEMA)$_n$−poly(EGDMA-*co*-DMAEMA) star polymers (PDMAEMA star polymer, hereafter). Similarly, the PAA star polymer was prepared by cross-linking the poly(*tert*-butyl acrylate) macroinitiators with divinylbenzene (DVB). The obtained poly(*t*BA)$_n$−poly(DVB-*co*-*t*BA) star polymer (P*t*BA star polymer, hereafter) was purified by fractionation to remove the linear chains before subsequent hydrolysis using trifluoroacetic acid in methylene chloride to form poly(AA)$_n$−poly(DVB-*co*-AA) star polymer (PAA star polymer, hereafter). ^{1}H NMR analysis of the hydrolyzed product verified that the proton peak from *tert*-butyl ester group was absent, indicating a complete hydrolytic process. The structural information on these star polymers is summarized in Table 1. The hydrodynamic diameter (D_h) of the star polymers was measured using a multiangle particle size analyzer (Brookhaven Instruments Corp.)

Table 1. Structural Information on Star Polymers Used in This Study

star polymer	$M_{w,star}$ (g/mol)	$M_{w,arm}$ (g/mol)	M_w/M_n (star)	M_w/M_n (arm)	n_{arm}[e]
PDMAEMA	2.16×10^5[a]	9670[a]	1.45[a]	1.21[a]	19
P*t*BA	1.55×10^5[c]	4120[b]	1.34[b]	1.16[b]	24
PAA	9.12×10^4[d]	2310[d]			24

[a] Weight-average molecular weight and polydispersity, measured by GPC in DMF with RI detector, calibrated with linear PMMA as standard. [b] Weight-average molecular weight and polydispersity, measured by GPC in THF with RI detector, calibrated with linear PS as standard. [c] Weight-average molecular weight, measured by GPC in THF with a MALLS detector. [d] Calculated molecular weight of PAA stars and arms based on complete deprotection of *tert*-butyl group. [e] Number-average value of the number of arms per star molecule ($n_{arm} = M_{w,star} \times arm_{wt\%}/M_{w,arm}$), where $arm_{wt\%}$ is the weight fraction of arms in the star polymer.

LbL Multilayer Film Assembly. All LbL films were assembled with a modified programmable Carl Zeiss HMS DS50 slide stainer. Typically, films were constructed on a silicon wafer with approximate size of 1 × 2 in.^{2}, which was treated in a plasma cleaner (Harrick Scientific Corp.) with O_2 plasma for 2 min prior to use. The substrate was then dipped into PDMAEMA star polymer solution (0.10 mg/mL) for 10 min and followed by three sequential rinsing steps with pH-adjusted water for 1 min each. Then the substrate was dipped into PAA star polymer solution (0.10 mg/mL) for 10 min and exposed to the same rinsing steps as described above. This cycle provides one bilayer of PDMAEMA star and PAA star polymer; here the notation of (PDMAEMA star/PAA star)$_1$ will be used, where the numeric subscript indicates the number of bilayers. Typically, the dipping process was repeated until films of 10 bilayers were obtained unless otherwise noted.

LbL Multilayer Film Characterizations. Film thickness was determined using a spectroscopic ellipsometer (Woolham Co.) at a fixed angle of 70° with varying wavelength of 300−900 nm. Thickness of the film was fit to the Cauchy model as reported.[5] The porosity of the film was calculated based on the Lorentz−Lorenz equation using a refractive index value obtained from ellipsometry.[6] Surface morphology of LbL film was observed by using Nanoscope IIIa AFM microscope (Digital Instruments, Inc.) in tapping mode in air. Root-mean-squared (rms) roughness was averaged from three different AFM images with a size of 5 × 5 μm^2. Large area surface morphology was collected with scanning electron microscopy (SEM, JEOL JSM-6060). Transmission measurements were performed using a UV−vis spectrophotometer (Varian Cary 600). Ionic (proton) conductivity values of LbL films were determined by impedance spectroscopy using an ac impedance analyzer (Solartron 1260) by sweeping the frequency from 100 kHz down to 10 Hz. 100 bilayers of star/star films were deposited on glass slides which were placed in a conductivity cell with platinum wires as the electrodes. Impedance measurements were then carried out in-plane (parallel to the substrate) in a humidity-controlled chamber (Electro-tech Systems, Inc.).

Results and Discussion

As mentioned earlier, star polymers with controlled structures were successfully synthesized via ATRP using the one-pot arm-

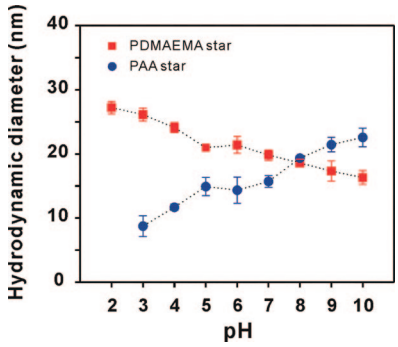

Figure 2. Hydrodynamic diameter (D_h) of PDMAEMA star (square) and PAA star (circle) polymers at varying pH conditions. The concentration of star polymers is 1.0 mg/mL. The values are averaged from three measurements. Note that the PAA star polymer precipitates out of the solution at pH 2.

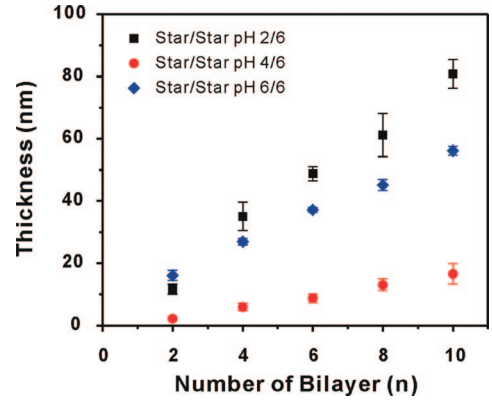

Figure 3. Growth curve of LbL assembled star/star multilayer films under different pH conditions. Ellipsometry was used to measure the film thickness at more than five different points on each sample. The pH of the PDMAEMA star solution was varied from 2 to 6, while that of the PAA star solution was fixed at pH 6.

first method (Scheme 1). First, linear PolyA macroinitiators (PolyA-Br) with controlled molecular weight and high chain-end functionality (active terminal bromines) were prepared by ATRP of the corresponding monomer (A). At certain conversion, divinyl cross-linker (X) was added, which copolymerized with the remaining monomer (A) and produced the targeted star polymers of arm-core type, $(PolyA)_n$−Poly(X-*co*-A), where Poly(X-*co*-A) represents the core of the star polymer and n is the average number of PolyA arms per star molecule. By changing the experimental parameters, such as the initial arm length of linear macroinitiators, the timing of addition of cross-linker, the added amount of cross-linker, and the chemical composition of monomer and cross-linker, the star structures can be significantly altered and different types of functionalities can be successfully introduced.

In this study, two types of star polymers with oppositely charged arms were synthesized and used for LbL film assembly (Table 1). The apparent weight-average molecular weight of the PDMAEMA star polymer is $M_{w,star} = 2.16 \times 10^5$ g/mol, determined by GPC in DMF with linear poly(methyl methacrylate) (PMMA) standards. On the basis of the weight fraction ($arm_{wt\%} = 84.6\%$) and the molecular weight of PDMAEMA arms ($M_{w,arm} = 9670$ g/mol) in the star polymer, the average arm number per PDMAEMA star molecule was calculated to be $n_{arm} = 19$ (Table 1). The absolute molecular weight of the fractionated P*t*BA star polymers before hydrolysis is $M_{w,star\text{-},MALLS} = 1.55 \times 10^5$ g/mol, determined by GPC in THF with a multiangle laser light scattering (MALLS) detector, and the averaged arm number per P*t*BA star molecule is $n_{arm} = 24$. After hydrolysis, the calculated molecular weight of the obtained PAA star polymer is $M_{w,star} = 9.12 \times 10^4$ g/mol, based on the complete deprotection of *tert*-butyl group. Furthermore, the averaged arm number for PAA star polymers is assumed to be the same as those from P*t*BA star polymer $n_{arm} = 24$ (Table 1).

As reported by others,[37,38] the effective pK_a of the star polymers varies from their linear counterpart due to the unique ionic confinement effect of star polymers, in which charged groups are packed in close proximity and high densities. This results in higher osmotic pressure inside the star polymers, which in turn leads to a partial reversal of acid−base ionization behavior. As a consequence, the pK_a values of the star polymers is shifted from that of their linear counterpart; for example, the pK_a of PDMAEMA decreases from 7.0 (linear) to 6.8 (star), and that of PAA changes from 5.8 (linear) to 6.4 (star) as determined from potentiometric titrations. In addition to the shift in pK_a values, the average hydrodynamic diameters (D_h) of the star polymers in solution vary significantly with pH as measured by dynamic light scattering (Figure 2). Since the side chains of star polymers are weak polyelectrolytes, the degree of ionization is highly dependent on the solution pH. When the pH is increased stepwise from 2 to 10, the D_h of PDMAEMA star polymer decreases from 27 to 16 nm. At low pH values, the PDMAEMA arms are fully stretched due to electrostatic repulsion between polyelectrolyte chains, whereas the repulsion decreases with pH increase, resulting in a gradual decrease in size. On the other hand, the D_h of PAA star polymer decreases from 23 to 9 nm from pH 10 to 3, corresponding to reduced electrostatic repulsion between polyelectrolyte chains. In contrast to its linear counterpart, the PAA star polymer has a limited solubility below pH 2, possibly due to the presence of the hydrophobic cross-linked core, which influences solubility without the contribution of charge stability provided by polyelectrolyte arms.

Since the side chains of both star polymers are weak polyelectrolytes, initially we have examined the assembly pH dependence of the LbL growth of PDMAEMA star and PAA star polymers. To maintain reasonable charges on the PAA star polymer, we have fixed the pH of the PAA star solution at 6 (near pK_a), while varying the pH of PDMAEMA star solution to tune the growth characteristics of multilayers. We investigated the assembly of PDMAEMA star and PAA star polymers based on three different conditions in this study, namely pH 2/6, 4/6, and 6/6 for PDMAEMA star/PAA star. The stepwise fabrication of star/star multilayer films was examined by spectroscopic ellipsometry. As shown in Figure 3, the growth of the star/star multilayers is linear with respect to the number of bilayers. Similar to the other weak polyelectrolyte systems, the assembly pH of the PDMAEMA star solution is critical in determining the final thickness and composition of the resulting multilayers. The average thickness of one bilayer—one PDMAEMA star and one PAA star polymer layer—corresponds to 7.7 nm (pH 2/6), 1.5 nm (pH 4/6), and 5.6 nm (pH 6/6). Although the average bilayer thickness does not necessarily reflect the internal structure of the multilayers, these values are significantly smaller than the expected thickness of bilayers based on the hydrodynamic size of the polymers as shown in Figure 2. Since the D_h of star polymers was measured in a swollen solution state, the smaller bilayer thickness values indicate that the star polymers are in a collapsed state on the charged surface, resulting in flattening of the stars on adsorption.

Interestingly, atomic force microscopy (AFM) measurements taken at the first stage of the LbL growth—only a single layer of the initial PDMAEMA star on silicon wafer—shows that the substrate is well covered by the globular structures of the star polymers (see Supporting Information). This is in contrast to the traditional LbL growth of linear polymers where the early

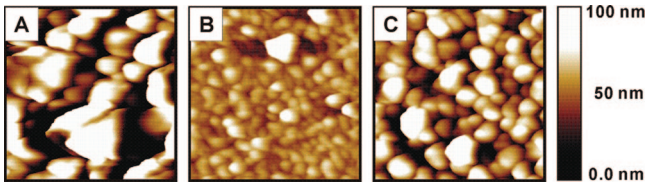

Figure 4. Representative AFM images of (PDMAEMA star/PAA star)$_{10}$ multilayer film prepared under (a) pH 2/6, (b) pH 4/6, and (c) pH 6/6 conditions. All images are in the scale of 1 μm × 1 μm × 100 nm.

stages of the deposition involve nucleation of island-like growth sites.

It is well-known that the pH of the deposition solution is critical in determining the degree of ionization of weak polyelectrolytes. For example, increasing the charge of a polymer results in the deposition of thinner layers due to the stretched chain conformation of the polymer in solution.[39] On the contrary, the pH 2/6 condition—fully charged PDMAEMA star polymer alternated with the highly charged PAA star—yields the thickest (star/star)$_{10}$ film (7.7 nm/bilayer). The pH of the dipping solution not only affects the ionization of polyelectrolytes in solution but also changes the ionization of the polyelectrolyte multilayer surface onto which adsorption occurs. Specifically, the PAA star polymers adsorbed on the film would undergo an extensive loss of ionization and subsequent aggregation on the surface when exposed to the dipping bath of PDMAEMA star polymer at pH 2. This results in a significant disruption of ionic cross-links and a precipitation of the star polymers while recruiting PDMAEMA star polymer from the solution. This effect is particularly enhanced because the PAA star polymer is not soluble in water solutions at pH 2. If one considers that the multilayer thin film surface is partially swollen with the surrounding aqueous solution, it is likely that the PAA stars adsorbed on the surface undergo conformational changes that lead to roughness and increased thickness of the film. The remaining two pH values, 4 and 6, do show an increase in thickness with higher pH that is consistent with the approach of pK_a of PDMAEMA.

As a control, we have assembled LbL films from linear PDMAEMA (M_n = 5000 g/mol) and PAA (M_n = 2000 g/mol) polymers using the same repeating unit concentration. Ten bilayers of linear PDMAEMA/linear PAA yield 2.70 (pH 2/6), 2.76 (pH 4/6), and 13.9 nm (pH 6/6) film, significantly thinner than star/star multilayers. In contrast to star polymers, linear polymers form smooth and continuous film and follow the general trend of film deposition behavior anticipated as described above with increasing thickness corresponding to decreasing charge density of positive polyelectrolytes. Moreover, their high molecular weight would prevent the interdiffusion of star polymers within a multilayer, which can be further supported by their linear growth trend observed in Figure 3, as opposed to exponential growth. The exponential growth is typically obtained with highly interpenetrating systems of polyelectrolyte multilayers.[40,41] It is important to note that the monomer unit concentrations we used in this experiment (0.10 mg/mL corresponds to 0.54 mM for PDMAEMA and 0.84 mM for PAA star, respectively) are considerably lower than the conventional LbL conditions in which the repeating unit concentration ranges around 10−20 mM. However, the control (linear PDMAEMA/linear PAA)$_{10}$ film prepared at pH 6/6 condition with a high monomer concentration (10 mM) still yields comparable thickness values (13.8 nm) to the same film prepared at low monomer concentration.

According to the AFM images shown in Figure 4, the surface morphology of all of the as-prepared star/star multilayer

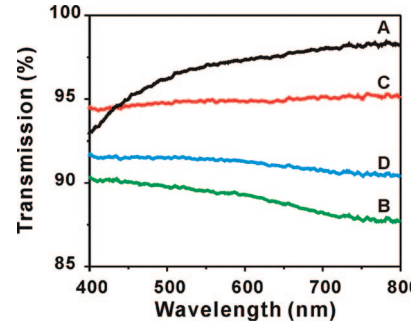

Figure 5. Transmission spectra of (PDMAEMA star/ PAA star)$_{10}$ multilayer film assembled on a glass slide: (A) star/star pH 2/6, (B) star/star pH 4/6, (C) star/star pH 6/6, and (D) uncoated glass. Multilayer coatings are on both sides of glass substrate. A quartz slide is used as a reference.

films exhibit nonuniform and rough structures. For example, 10 bilayer films of both pH 2/6 and pH 6/6 yield significantly rough films with root-mean-squared (rms) roughness of ca. 65 and 25 nm, respectively (averaged over 25 μm^2 area). The grain size of these films is approximately 150−250 nm, which could be the result of interconnected star polymer aggregations. On the contrary, the pH 4/6 film is relatively smoother with an rms roughness of 13 nm for (star/star)$_{10}$ multilayer, which is the thinnest among the star/star multilayers prepared. These trends are consistent with the film thickness observations discussed above. The roughness values of all of the star/star multilayers are in general significantly higher than those films composed of linear PDMAEMA/PAA polyelectrolytes (0.8−1.0 nm). We attribute this to the unique structural conformation of the star polymers. Unlike linear polyelectrolytes, star polymers may not experience a high degree of interpenetration and complexation with each other due to topological constraints. Instead, their polymeric arms may partially interdigitate with each other to form ionic cross-links within multilayers. It should be noted that for the same reasons this effect is greatly impacted by kinetics because the organization of these star systems is considerably kinetically hindered. For this reason, we have observed structural reorganization and the smoothening of films that were assembled and later exposed to solutions at the same pH condition as assembly for extended time periods. This annealing effect indicates nonequilibrium states of dipping conditions. For example, when the (star/star)$_{10}$ film prepared at pH 6/6 was exposed to pH 6 solution for 30 min, the rms roughness decreased from 25 to 7 nm. This suggests that the as-assembled film is in a kinetically trapped state in which high molecular weight and structurally restricted star polymers need a considerably greater amount of time to arrange into more favorable conformations following adsorption. A control experiment with an increased dipping time (from 10 to 30 min per each layer deposition) showed significantly enhanced smoothness of the film as noted from the decrease in rms roughness value from 25 to 4 nm for (star/star)$_{10}$ film prepared at pH 6/6.

For the films adsorbed with 10 min cycles, the topological constraints of the star systems would leave an interstitial void volume within the multilayer and lead to the formation of pores within the multilayer. This phenomenon has been similarly reported for multilayers composed of inorganic nanoparticles[5] and block copolymer micelles.[6] To test this concept in the all-star multilayers, we have further explored the possibility of molecular to nanometer scale porosity using ellipsometry because the presence of void volume within the multilayer would decrease the effective refractive index of the star/star films. The refractive indices of (star/star)$_{10}$ films are 1.11 (pH 2/6), 1.43 (pH 4/6), and 1.21 (pH 6/6) where the corresponding porosity of each film is calculated to be

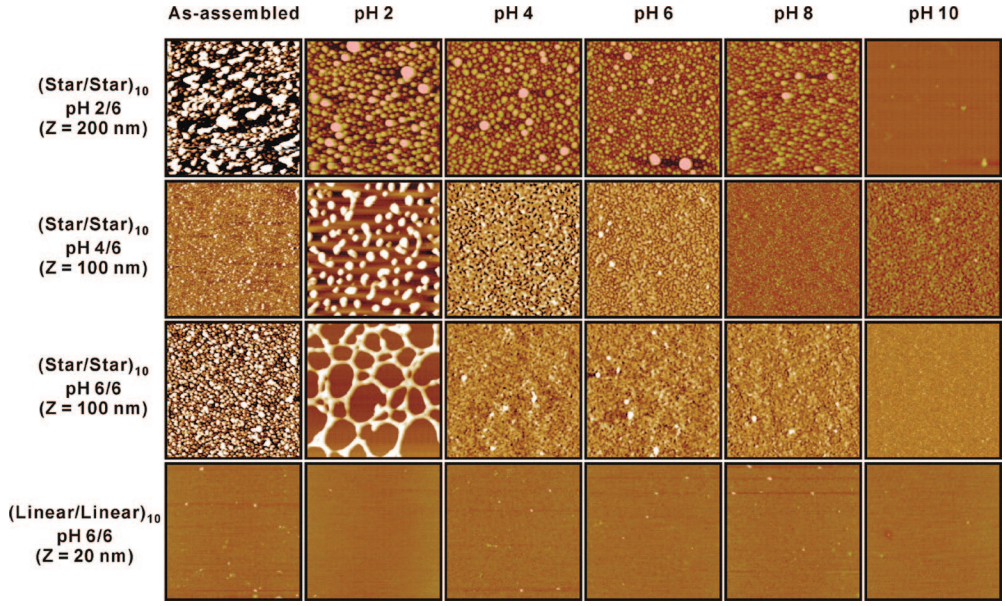

Figure 6. Representative AFM images of a (PDMAEMA star/PAA star)$_{10}$ multilayer film treated at varying pH conditions. (PDMAEMA linear/PAA linear)$_{10}$ film was used as a control. All images are in height mode with dimensions of 5 × 5 μm^2. All films are dipped for 30 min at varying pH solutions for post-treatment and gently dried with air. Note that the z-scale of pH 2 treated (star/star)$_{10}$ film of pH 6/6 is 300 nm.

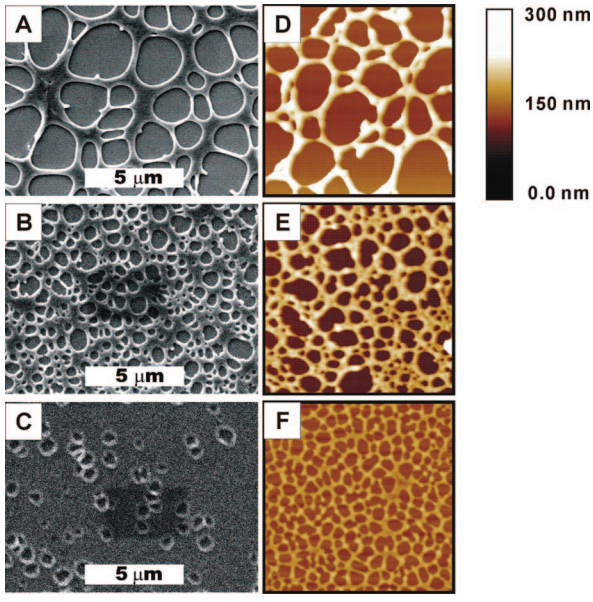

Figure 7. Morphology changes of (star/star)$_{10}$ film prepared at pH 6/6 under different pH treatment. (A−C) SEM and (D, F) AFM images of the film after treatment in (A, D) pH 2, (B, E) pH 2.5, and (C, F) pH 3 solutions for 30 min. All AFM images are in 5 × 5 μm^2.

72.3%, 8.4%, and 47.6%, respectively, based on the Lorentz−Lorenz effective medium equation[6]

$$P = \frac{2(n_o^2 - n_f^2)}{(n_o^2 - 1)(n_f^2 + 1)} \quad (1)$$

where n_o, n_f, and P are the refractive index of the star polymers (average of PDMAEMA and PAA stars), the star/star multilayer film (measured from ellipsometry), and the porosity, respectively. Overall, we find that the thickness, roughness, and porosity of the star/star multilayer films from the different pH conditions all exhibit similar trends.

On the basis of the highly nanoporous structure formed from star/star multilayer films, we have investigated the antireflective property of these films.[42] Figure 5 shows the light transmission of the star/star multilayer film deposited on a glass slide prepared with varying assembly pH values. Relatively high light transmission is observed for the (star/star)$_{10}$ film with 97.0% (pH 2/6) and 94.9% (pH 6/6) at 550 nm. However, the (star/star)$_{10}$ film prepared from pH 4/6 (curve B) exhibited the lowest transmission of 89.5% at 550 nm, even lower than that of the blank glass substrate (curve D), which is due to the low degree of porosity in the multilayer. The film has not antireflective property, and surface roughness may have actually contributed to surface scattering, thus reducing the percent transmission below that of the original glass slide.

Several researchers have previously demonstrated that the multilayer assemblies fabricated from certain weak polyelectrolytes can undergo changes in surface morphology and internal structure upon exposure to external conditions such as pH, temperature, and ionic strength, which disrupt the internal cross-links present in the multilayers.[43,44] For example, Rubner and co-workers have reported the porosity transition of polymeric multilayers prepared from weak polyelectrolytes of poly(allylamine hydrochloride)/poly(acrylic acid) (PAH/PAA), which phase separated into micro- and nanoporous structures upon exposure to a selected relatively narrow pH range.[44] Similarly, our group has observed the generation of asymmetric porous film from linear poly(ethylenimine)/poly(acrylic acid) (LPEI/PAA) multilayer upon treatment with acidic pH ranges.[45]

Likewise, to explore the conditions under which the star/star multilayer film would undergo pH-responsive behavior, we investigate the structural transitions upon exposure to a wide range of pH solutions from 2 to 10. Following the assembly of the (star/star)$_{10}$ film under different conditions, the multilayers were immersed into solutions of different pH ranges for 30 min, and then the morphology was examined by using AFM in tapping mode (Figure 6). In general, all of the star/star multilayer films undergo structural transitions upon exposure to different pH conditions. As a clear contrast, the control linear/linear multilayer film did not show any noticeable structural change or porosity transition upon pH treatment.

There is no clear morphological transition observed in films prepared at pH 2/6 condition; this is consistent with the observation of unusually rough and thick films at this pH and the concept that the PAA becomes aggregated on the surface during the dipping process due to low solubility when the top

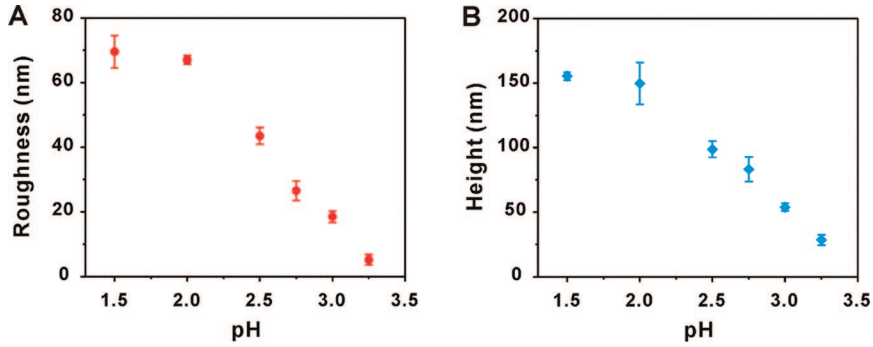

Figure 8. Structural changes of $(star/star)_{10}$ film prepared at pH 6/6 upon post-treatment. (A) rms surface roughness and (B) ridge height changes of the film with varying pH. All values are obtained from AFM measurement of three different images with a size of 5×5 μm^2.

surface of the film is immersed in the pH 2 PDMAEMA solution. At pH 2, the film would not have the mobility needed for any annealing or pH-induced rearrangements, and at higher pH values, the driving force for rearrangement is not sufficient for a film built under the most acidic conditions.

In contrast to pH 2/6 film, both the pH 4/6 and pH 6/6 films undergo considerable swelling and structural reorganization with pH changes, most notably at the pH 2 condition (Figure 6). As more ionic cross-links within multilayers are present in both films compared to pH 2/6 film, they yield rapid and extensive spinodal-type decomposition with post-pH treatment. Basic conditions appear to completely destabilize electrostatic interactions that hold the films together, as PDMAEMA stars become completely uncharged and PAA stars become highly negatively charged; in all cases, almost no multilayer films are left on the substrate after exposure to pH 10.

In particular, we have further investigated the morphology transitions of $(star/star)_{10}$ films prepared at pH 6/6 under acidic conditions (Figure 7). While other star/star films show relatively gradual changes in the morphological transitions with pH, the film prepared at pH 6/6, when exposed to acidic conditions, shows the most significant structural reorganization of the components of these films over large length scales. We observed that the $(star/star)_{10}$ film prepared at pH 6/6 produced an open pore membrane-like structure upon incubation in pH solutions below pH 3.5.

For example, the average height of the ridges shown in Figure 7A (and 7D) is ca. 150 nm (also in Figure 8B). This value is significantly greater than the thickness of the film prior to pH treatment (56 ± 1.4 nm), suggesting that the star polymer flowed into or accumulated in these regions of the film during the phase transformation. A simple surface scratch experiment revealed that the bare silicon wafer is exposed after the pH 2 treatment. Moreover, we found that these structural transitions are irreversible and very sensitive to the pH of the solutions. While the pH 3.25 solution produced small holes of 30 nm height, these holes become large enough to form interconnected membrane-like structures upon incubation in a solution of pH below 3 (Figure 8). The structure generated from exposure to pH 1.5 is similar to what is observed in the case of pH 2. We can relate the underlying chemical basis for the unique morphological changes with respect to the pH-dependent ionization of the individual components of the multilayers. When the $(star/star)_{10}$ films are exposed to acidic pH, the PDMAEMA star polymer would acquire more protons from the solution, while a substantial portion of PAA star polymer would become protonated. This change will extensively disrupt the ionic cross-links that were present in the multilayer, resulting in significant changes in the internal structure of the star/star multilayers. This process yields a spinodal-type decomposition with the two polymers, as described by Rubner and co-workers,[44] leaving an insoluble polymer precipitate on the substrate. We have also confirmed that this morphological transition is not simply due to the drying process by taking the optical microscope image of the film in the buffer solution (data not shown).

The FT-IR spectra of the $(star/star)_{10}$ film after the pH treatment illustrate the molecular basis of the structural changes associated with the pH treatment (Figure 9). Two pronounced peaks are observed from the FT-IR spectra: one from carboxylate peak (1594 cm^{-1}) of the PAA star polymer and one from carbonyl group (1733 cm^{-1}) both present in PDMAEMA star and PAA star polymers. Moreover, the contribution from the amine peak (1618 cm^{-1}) of protonated PDMAEMA star polymers is deconvoluted by the Gaussian fitting process. On the basis of this method, we found that the fraction of charged carboxylate group (1594 cm^{-1}) to carboxylic acid group (1733 cm^{-1}) of PAA star polymer decreases sharply below pH 2.5 exposure, although we could not find the exact contribution from individual polymers due to the considerable peak overlap. The sharp transition between pH 2 and 2.5 suggests a considerable structural change occurring at this pH range, which was previously reported as the effective pK_a of PAA polymers existent within a multilayer. It has been similarly observed that the effective pK_a of the PAA polymers within a multilayer is significantly lower than the value measured in solution (pK_a of PAA in the solution is reported in the range of 4.5−6).[44,45] It is worth noting that a PAA star polymer has a similar transition to the linear PAA polymer in PAH/PAA or LPEI/PAA, albeit there is a slight shift of pK_a values. This result corroborates the data obtained from the AFM experiments with respect to the relative changes in both rms roughness and height of the film after post-pH treatment (Figure 8). It is important to mention that these star multilayer systems undergo transitions at conditions when their equivalent linear systems do not. We believe this is due to the increased mobility of their compact structure, lowered number of entanglements and degree of interpenetration, and the reduced number of effective ionic cross-links gained due to topological constraints.

Impedance spectroscopy has proven to be an effective tool to characterize the solid-state electrolyte properties of LbL assembled thin films.[16] It can provide valuable morphological information by quantifying the mobility of ions through the domains and subdomains of these ionically cross-linked systems. Since the studied star/star polymer films bear proton conducting functionalities such as amine and carboxylate groups, the overall proton conductivity of the LbL assembled composite will be affected by the packing density of the ionic network, number of free ionic groups, and presence of interstitial volume and ion-rich domains. We have recently shown that the subtle changes in film composition and morphology can have major effects on ionic conductivity.[46] To measure ionic conductivity of star/star films and explore the effects of post-pH treatment, we have assembled 100 bilayers pH 6/6 films on glass slides and placed them in a two-probe conductivity cell connected to

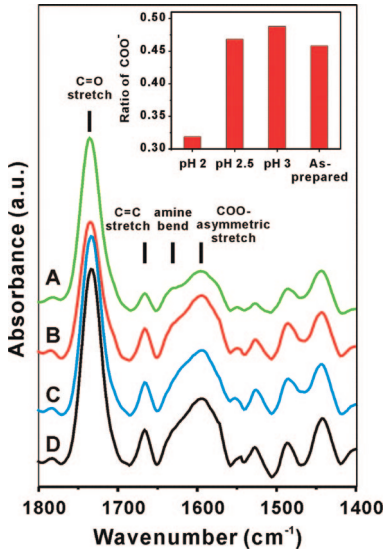

Figure 9. FT-IR spectra changes of $(star/star)_{10}$ film prepared at pH 6/6 upon post-treatment. (A) pH 2, (B) pH 2.5, (C) pH 3, and (D) as-prepared film. (inset) Fraction of carboxylate peak calculated from FT-IR spectra. Spectra are vertically shifted for clarity. The ratio of carboxylate peak at 1594 cm^{-1} was calculated from the sum of absorbance at 1733 cm^{-1} (C═O stretching) and 1618 cm^{-1} (N−H bending). Peak at 1666 cm^{-1} (C═C stretching, unreacted benzyl group from cross-linked PAA star core) was used as an internal reference.

an ac impedance analyzer. Initial in-plane resistance measurements with 1.0 cm electrode spacing show that the conductivity of an untreated film is very high (<0.001 mS/cm at relative humidity of 98% at 25 °C, beyond the detection limit of analyzer, no plasticizer used) possibly due to the high ionic cross-linking density and lack of free proton carriers. However, when the films are exposed to low-pH solutions such as pH 3 and pH 2, the proton conductivity values are measured to be 0.051 and 0.034 mS/cm, respectively. These preliminary results show that the post-pH treatment increases the bulk ionic conductivity possibly through the formation of pores within the LbL film.

Summary and Perspectives

In summary, we have demonstrated the synthesis of star polymers with a controlled structure via the ATRP method and their pH-responsive characteristics in multilayer thin films. By taking advantage of versatile layer-by-layer assembly techniques, we have assembled the multilayers of star polymers based on electrostatic interaction between their polyelectrolyte arms. The assembled star/star multilayer films exhibit nonuniform and porous structures, which result from the architecture and high molecular weight of star polymers as compared to conventional linear polyelectrolytes. The solution pH of the star polymers is found to be the main parameter to tune the thickness, porosity, and refractive index of the resulting star/star multilayers. Moreover, as-assembled films undergo extensive structural reorganization upon post-treatment with different pH conditions due to the highly pH-sensitive nature of star polymers. With their compact structure and low degree of ionic cross-links, these star polymers exhibit characteristic behaviors that are absent in their linear counterparts. Their morphological changes are characterized by AFM, SEM, and FT-IR. In addition, we have observed an enhanced ionic conductivity of star/star multilayer upon post-pH treatment. We are currently expanding the scope of star/star polymer multilayer assembly with different molecular weights, number of arms, and different core sizes. We anticipate that with their interesting architectures and high degree of functionalities these star polymers will provide a new avenue for the LbL assembled multilayer thin films. These films can then be used in potential applications such as vehicles for drug delivery, porous membranes, and pH-responsive surface engineering materials.

Acknowledgment. We thank Dr. Jung Ah Lee for SEM images and Dr. Hyung-il Lee for providing linear PDMAEMA and PAA. The financial support from the Institute for Soldier Nanotechnologies (ISN), NSF (DMR-05-49353), and the CRP Consortium at Carnegie Mellon University is greatly appreciated. H. Gao acknowledges the support from McWilliams Fellowship at Carnegie Mellon University.

Supporting Information Available: Experimental details of star polymer synthesis and an additional AFM image. This material is available free of charge via the Internet at http://pubs.acs.org.

References and Notes

(1) Decher, G. *Science* **1997**, *277*, 1232.
(2) Caruso, F. *Adv. Mater.* **2001**, *13*, 11.
(3) Peyratout, C. S.; Dahne, L. *Angew. Chem., Int. Ed.* **2004**, *43*, 3762.
(4) Hammond, P. T. *Adv. Mater.* **2004**, *16*, 1271.
(5) Lee, D.; Rubner, M. F.; Cohen, R. E. *Nano Lett.* **2006**, *6*, 2305.
(6) Cho, J. H.; Hong, J. K.; Char, K.; Caruso, F. *J. Am. Chem. Soc.* **2006**, *128*, 9935.
(7) Tsukruk, V. V. *Adv. Mater.* **1998**, *10*, 253.
(8) Khopade, A. J.; Caruso, F. *Nano Lett.* **2002**, *2*, 415.
(9) Mamedov, A. A.; Kotov, N. A.; Prato, M.; Guldi, D. M.; Wicksted, J. P.; Hirsch, A. *Nat. Mater.* **2002**, *1*, 190.
(10) Lvov, Y.; Ariga, K.; Ichinose, I.; Kunitake, T. *J. Am. Chem. Soc.* **1995**, *117*, 6117.
(11) DeLongchamp, D.; Hammond, P. T. *Adv. Mater.* **2001**, *13*, 1455.
(12) Lowman, G. M.; Hammond, P. T. *Small* **2005**, *1*, 1070.
(13) Tang, Z. Y.; Wang, Y.; Podsiadlo, P.; Kotov, N. A. *Adv. Mater.* **2006**, *18*, 3203.
(14) Wood, K. C.; Zacharia, N. S.; Schmidt, D. J.; Wrightman, S. N.; Andaya, B. J.; Hammond, P. T. *Proc. Natl. Acad. Sci. U.S.A.* **2008**, *105*, 2280.
(15) Kim, B. S.; Park, S. W.; Hammond, P. T. *ACS Nano* **2008**, *2*, 386.
(16) Lutkenhaus, J. L.; Hammond, P. T. *Soft Matter* **2007**, *3*, 804.
(17) Lynn, D. M. *Soft Matter* **2006**, *2*, 269.
(18) Hadjichristidis, N.; Pitsikalis, M.; Pispas, S.; Iatrou, H. *Chem. Rev.* **2001**, *101*, 3747.
(19) Mishra, M.; Kobayashi, S. *Star and Hyperbranched Polymers*; Marcel Dekker: New York, 1999.
(20) Matyjaszewski, K.; Davis, T. P. *Handbook of Radical Polymerization*; Wiley: Hoboken, 2002.
(21) Matyjaszewski, K. *Controlled/Living Radical Polymerization. From Synthesis to Materials*; American Chemical Society: Washington, DC, 2006.
(22) Braunecker, W. A.; Matyjaszewski, K. *Prog. Polym. Sci.* **2007**, *32*, 93.
(23) Wang, J. S.; Matyjaszewski, K. *J. Am. Chem. Soc.* **1995**, *117*, 5614.
(24) Matyjaszewski, K.; Xia, J. *Chem. Rev.* **2001**, *101*, 2921.
(25) Kamigaito, M.; Ando, T.; Sawamoto, M. *Chem. Rev.* **2001**, *101*, 3689.
(26) Ueda, J.; Matsuyama, M.; Kamigaito, M.; Sawamoto, M. *Macromolecules* **1998**, *31*, 557.
(27) Matyjaszewski, K.; Miller, P. J.; Fossum, E.; Nakagawa, Y. *Appl. Organomet. Chem.* **1998**, *12*, 667.
(28) Matyjaszewski, K.; Miller, P. J.; Pyun, J.; Kickelbick, G.; Diamanti, S. *Macromolecules* **1999**, *32*, 6526.
(29) Gao, H.; Matyjaszewski, K. *Macromolecules* **2008**, *41*, 1118.
(30) Gao, H.; Matyjaszewski, K. *Macromolecules* **2006**, *39*, 4960.
(31) Whittaker, M. R.; Urbani, C. N.; Monteiro, M. J. *J. Am. Chem. Soc.* **2006**, *128*, 11360.
(32) Xia, J. H.; Zhang, X.; Matyjaszewski, K. *Macromolecules* **1999**, *32*, 4482.
(33) Zhang, X.; Xia, J. H.; Matyjaszewski, K. *Macromolecules* **2000**, *33*, 2340.
(34) Baek, K. Y.; Kamigaito, M.; Sawamoto, M. *Macromolecules* **2001**, *34*, 215.
(35) Gao, H.; Matyjaszewski, K. *Macromolecules* **2006**, *39*, 3154.
(36) Yang, S.; Zhang, Y.; Wang, C.; Hong, S.; Xu, J.; Chen, Y. *Langmuir* **2006**, *22*, 338.
(37) Connal, L. A.; Li, Q.; Quinn, J. F.; Tjipto, E.; Caruso, F.; Qiao, G. G. *Macromolecules* **2008**, *41*, 2620.
(38) Plamper, F. A.; Becker, H.; Lanzendorfer, M.; Patel, M.; Wittemann, A.; Ballauf, M.; Muller, A. H. E. *Macromol. Chem. Phys.* **2005**, *206*, 1813.

(39) Shiratori, S. S.; Rubner, M. F. *Macromolecules* **2000**, *33*, 4213.
(40) Picart, C.; Mutterer, J.; Richert, L.; Luo, Y.; Prestwich, G. D.; Schaaf, P.; Voegel, J. C.; Lavalle, P. *Proc. Natl. Acad. Sci. U.S.A.* **2002**, *99*, 12531.
(41) Yoo, P. J.; Zacharia, N. S.; Doh, J.; Nam, K. T.; Belcher, A. M.; Hammond, P. T. *ACS Nano* **2008**, *2*, 561.
(42) Hiller, J.; Mendelsohn, J. D.; Rubner, M. F. *Nat. Mater.* **2002**, *1*, 59.
(43) Li, Q.; Quinn, J. F.; Caruso, F. *Adv. Mater.* **2005**, *17*, 2058.
(44) Mendelsohn, J. D.; Barrett, C. J.; Chan, V. V.; Pal, A. J.; Mayes, A. M.; Rubner, M. F.*Langmuir* **2000**, *16*, 5017.
(45) Lutkenhaus, J. L.; McEnnis, K.; Hammond, P. T. *Macromolecules* **2008**, *41*, 6047.
(46) Argun, A. A.; Ashcraft, J. N.; Hammond, P. T. *Adv. Mater.* **2008**, *20*, 1539.

MA801812V